Application of Electric Voltages for Improved Protection of MgO Refractory Materials

EIRICH AWARD ´09

R.K. Sauerbrey, G. Mori, Ch. Majcenovic, H. Harmuth

MgO electrodes were polarized at voltages of up to 10 V in a synthetic lime-alumina-silicate slag at 1400 °C and at 5 A in synthetic fayalite slag at 1250 °C. Cathodic corrosion protection was obtained in both cases, requiring voltages of min. 8 V and approx. 1 V, respectively. Protection was achieved through rapid migration of mobile Ca^{2+} ions and their accumulation at the slag/electrode interface in the first case and the electrochemical reduction of FeO in the latter case.

①	Graphite crucible
②	Molten slag
③	Al_2O_3 tube
④	Carbon fibre rods
⑤	MgO samples
⑥	Thermocouples
⑦	Gas inlets
⑧	Al_2O_3 pedestals
⑨	Electric furnace
⑩	Al_2O_3 fibre cover
⑪	Potentiostat
⑫	Voltmeter

Fig. 1 Scheme of the test furnace

1 Introduction

Refractory products primarily consisting of MgO are widely used in heavy industries under severe conditions, which curtail the lifetime of these ceramic materials. Often a combinatory attack of corrosion, mechanical erosion and thermal loads can be observed. Refractory wear in metallurgical vessels is very often found to be the most serious at the interfaces of melt wetted lining areas, where electrochemical corrosion could well contribute to the overall corrosion extent, because the latter corrosion type only occurs at these three-phase boundaries [1–7]. Due to this, electrochemical corrosion phenomena in the heavy industries were investigated as early as 1957 by De Jong [8]. Following research activities demonstrated that the application of electric voltages can potentially cause a significant reduction of refractory dissolution at the three-phase boundaries [1, 4, 9, 10], although the polarity of a protective potential appears to be highly dependent on the particular system. An influence of applied voltages on the three-phase boundary phenomenon of Marangoni convection was assumed by Monaghan et al. [11]. This local effect was thoroughly investigated [12–17] and is driven by gradients in surface tension due to the dissolution of ceramic materials. The convective motion can be either accelerated or counteracted by electrically induced ion migration, which is dependent on voltage height and melt composition. Electric voltages can also positively affect the penetration of melts into refractory matrices by increasing the contact angle between refractories and melts [9, 10, 12–14, 17–21]. At contact angles > 90° the wettability of refractories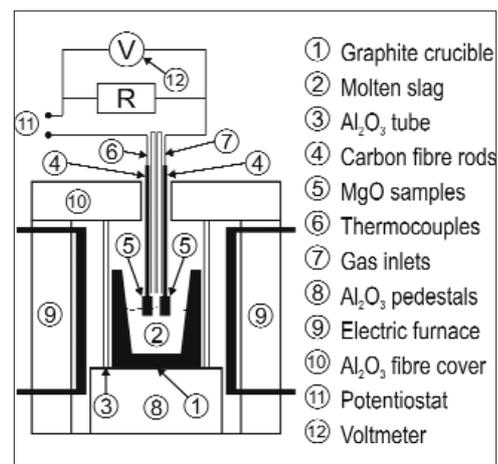 is considerably lowered resulting in a massive reduction of local corrosion. Minimized melt infiltration depths were thus achieved by the application of applied voltages [9, 10, 22–24].

The ionic nature of melts at processing temperatures [5, 25–29] also allows the migration of charged slag components in electric fields, which was already used to improve corrosion protection and slag refinement [22, 23, 26, 30–33].

The first part of the work presented below originally expanded on the anodic polarization experiments of *Kriksunov* et al. [34] with high-alumina refractories in molten lime-alumina silicates. The protective effect was argued to stem from the creation of a Ca^{2+} deficient zone, which prevented the formation of low-melting CAS phases and considerably slowed refractory dissolution. Due to the fact that Al_2O_3 shows a chemically more acidic behavior than MgO, the cathodic polarization should prove more beneficial for the basic oxide MgO. This has already been demonstrated in an earlier publication by the authors of this work [35], but here further results are presented. The second part deals with electrochemically induced reactions derived from the results published by *Warczok* et. al. [32, 33].

DI DDr. R.K. Sauerbrey, Technology Center, RHI AG, 8700 Leoben, Austria

Ao. Univ.-Prof. DI Dr. G. Mori, CD-Laboratory of Localized Corrosion, University of Leoben,
8700 Leoben, Austria

Dr. Ch. Majcenovic, Technology Center, RHI AG, 8700 Leoben, Austria

O. Univ.-Prof. DI Dr. H. Harmuth, Chair of Ceramics, University of Leoben,
8700 Leoben, Austria

Corresponding author:
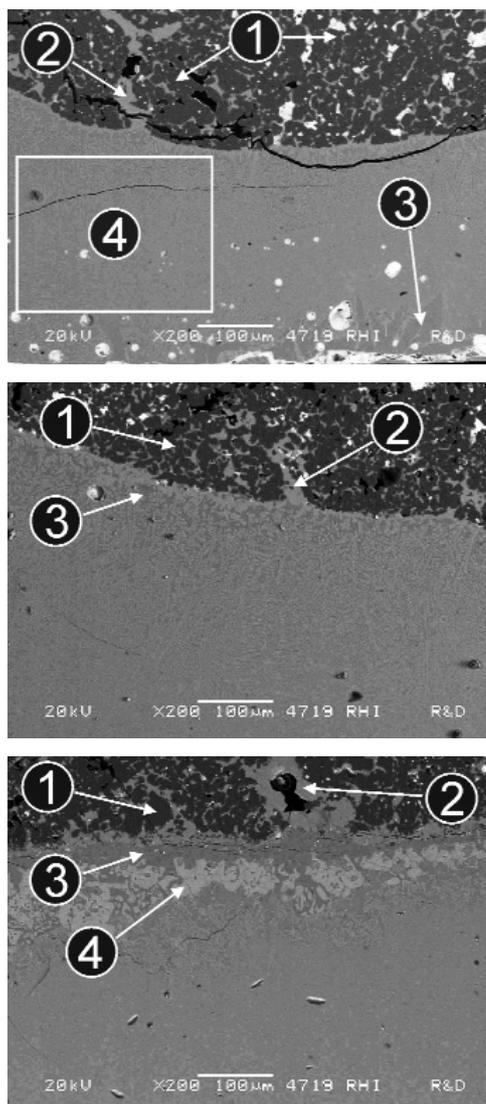E-mail: robert.sauerbrey@rhi-ag.com

Fig. 2 BSE-SEM micrographs of the slag-MgO interfacial regions after polarization in CAS slag at 1400 °C with 8 V for a) 3 h (reference sample), b) 1 h (anode) and c) 3 h (cathode). Numbers refer to Table 1

In both cases it is demonstrated that the cathodic polarization of MgO electrodes indeed has a protective effect by causing the formation of solid barrier layers, effectively preventing corrosion.

2 Experimental procedure

Due to the investigation of the effect of applied voltages on the dissolution behavior of MgO, a cathode, an anode and an unpolarized reference sample were present in the experimental setup according to standard practice [1, 4, 9–11, 24, 31–34, 36, 37]. The electrodes were lowered into the melt without preheating and the distance between anode and cathode as well as the immersion

depth were 3 mm. The voltage was switched on before insertion to prevent unnecessary slag infiltration. Due to the small distance between electrodes and the high electric slag conductivities at 1400 °C of 0,12 Ω^{-1} cm^{-1} for the CAS slag [38] and 2,50 Ω^{-1} cm^{-1} for the fayalite slag [39] the iR-drop was considered to be negligible. A p1050-P potentiostat from *Plating Electronic* was used as power source. The duration of experiments varied, because anodes tended to dissolve rapidly. After removal and air cooling all samples were prepared for SEM/EDS-analysis by sectioning, grinding and polishing using standard procedures. Experiments were executed under Ar/4 % H$_2$ atmosphere at 1400 °C in a self-constructed test furnace (Fig. 1).

The raw material for MgO electrodes was *Nedmag* NM30-fines with > 98 % purity, which was shaped into a brick with a pressure of 140 MPa and subsequently fired at 1650 °C. After firing an apparent density of 2,65 g/cm^3 and an open porosity of 25,3 % were achieved. Fifty percent of the pores were < 4,0 µm and 90 % < 6,5 µm. Cylinders with 80 x 10 mm^2 were drilled out and cut into 15-mm samples using a diamond saw. The face sides were polished with a di-

amond-coated disc. From prior experiments it was known that drying at 160 °C prior to drilling a 10 x 4 mm^2 blind-hole in one of the electrode faces prevented bursting. The electrodes were fastened to 4 mm diameter carbon fibre rods from *Graphtek* by applying a drop of standard resole resin into the blind-hole and hardening at 160 °C. Electric conductivity was achieved by in-situ coking during the exposition in the test furnace.

The CAS-slag with 48,5 % CaO, 40,0 % SiO$_2$ and 11,5 % Al$_2$O$_3$ was composed of CaCO$_3$, quartz sand and calcined alumina with purities > 98%. This composition resulted in a low liquidus temperature of approx. 1315 °C and a slag basicity of CaO/(SiO$_2$ + Al$_2$O$_3$) = 0,94 meaning that the SiO$_2$-rich slag was prone to solidify in glassy state. Slag preparation commenced with a homogenization step for 1 h in a ball mill, followed by overnight calcination at 900 °C. After compaction in a small hydraulic press the pellets were immediately pre-melted in clay-bound graphite crucibles (capacity approximately 200 cm^3) from *Goebel*. The homogenized slag was then used in the same crucibles for the experimental work. The stoichiometric fayalite slag was pre-melted in an electric arc furnace, subsequently crushed and thus

Tab.1 Phase compositions at the reference sample and the cathode after a 3 h polarization in CAS slag with a voltage of 8 V; the anode was polarized for 1 h only

	Al$_2$O$_3$	CaO	MgO	SiO$_2$	C/S	Calc. phase composition
	[mass-%]	[mass-%]	[mass-%]	[mass-%]		[mass-%]
Reference sample						
1	-	-	100,0	-	-	100 M
2	-	51,0	12,3	36,7	1,39	100 C$_3$MS$_2$ + 0 C$_2$MS$_2$ + 0 CMS
3	19,9	39,7	3,5	36,9	1,08	65 Mel (65 C$_2$AS, 35 C$_2$MS$_2$) + 20 CS + 15 An
4	10,3	45,9	5,9	37,9	1,21	C$_3$MS$_2$ + Mel (area analysis)
Anode						
1	-	-	100,0	-	-	100 M
2	-	51,9	11,5	36,6	1,42	100 C$_3$MS$_2$ + 0 C$_3$S$_2$ + 0 C$_2$S
3	19,7	32,8	9,4	38,1	0,86	65 CS + 25 Sp (95 MA) + 10 CMS$_2$
Cathode						
1	-	-	100,0	-	-	100 M
2	-	52,2	10,9	36,9	1,42	90 C$_3$MS$_2$ + 5 C$_3$S$_2$ + 5 C$_2$S
3	27,5	42,3	3,1	27,1	1,56	95 Mel (75 C$_2$AS, 25 C$_2$MS$_2$) + 5 C$_2$S
4	-	64,8	-	35,2	1,84	95 C$_2$S + 5 C$_3$S$_2$

needed no further preparation. Alumina crucibles were used for those experiments.

3 Results
3.1 CAS slag

A slag basicity of 0,94 is considered to be very aggressive to basic refractory materials, but it allowed for short experiments and thus for a quick assessment of polarization effects in this electrolyte. A common evaluation procedure is the measurement of infiltration depths or corroded sample areas [9–11, 24, 34]. In practice, most electrodes exhibited one or more micro-cracks, which facilitated melt infiltration into the material. Consequently, infiltration depths were not measured. Experiments in CAS slag were carried out at voltages up to 10 V between anode and cathode. Below 8 V however, there was no discernible difference between the polarized samples and the reference in terms of appearance and phase composition as was demonstrated in [35]. The most pronounced material dissolution at lower voltages inevitably occurred at the three-phase boundary. At the boundary of the unpolarized sample merwinite crystals and melilite matrices were identified in addition to still uncorroded MgO grains (Fig. 2a). The dissolution of the reference sample proceeded along the crystal boundaries of periclase as cited in [34].

Table 1 demonstrates that the gross slag composition in the interfacial region of the reference sample was nearly identical to the nominal bulk composition.

A further voltage increase from 6 to 8 or 10 V resulted in pronounced differences between all samples, one of which was the utter dissolution of the anode after just 1 h. EDS analysis of the area depicted in Fig. 2b confirmed that the slag infiltrated in the anode consisted of merwinite only (Tab. 1). This phase was again detected in a spinel matrix with a rather low CaO content. The significant acceleration of anode dissolution was presumably caused by a decrease of interfacial tension at the slag-refractory boundary as implicated in [9, 24].

At the cathode, negligible corrosion and infiltration (Fig. 2c) due to the formation of a solid slag layer was observed (Fig. 3).

This protective layer rapidly disintegrated after cooling, which corresponded to the well-known decay due to the temperature-dependent modification changes of dicalcium
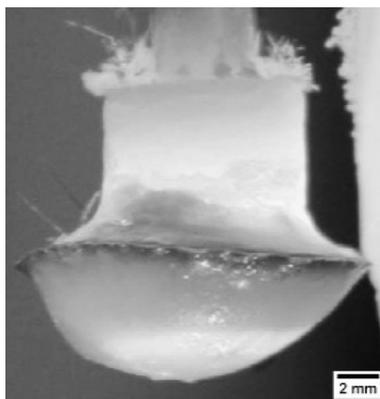

Fig. 3 Cathode with adhering CAS slag immediately after polarization with 8 V for 3 h, 1400 °C

silicate with an associated volume expansion of 12 % [40]. In the pores at the very edge of the cathode traces of merwinite (Tab. 1) were found (Fig. 2c). Moving outwards from the electrode a melilite layer with a pronounced deficiency in SiO_2 and a very high Al_2O_3 content followed. The next layer consisted of a several hundred micron thick layer consisting of almost pure C_2S. Finally, a two phase region made of dicalcium silicate and melilite made up the rest of the solidified slag layer. Still farther out the presence of silicon metal was visually determined in the slag.

3.2 Fayalite slag

Whereas polarization experiments in CAS slag were carried out potentiostatically, this was not possible with the approx. 20 times more conductive fayalitic slag system [38, 39]. The observed current easily reached the maximum output of 5 A of the power source, which forced a galvanostatic process control. The resulting voltage remained nearly constant at approx. 1 V throughout the experiments. Despite the low voltage there was a protective effect similar to the experiments in CAS slags at min. 8 V, although the consistency of the solidified slag layer varied. Contrary to the complete solidification described above the fayalitic slag layer retained a certain viscosity resulting in a typical downward facing cone (Fig. 4).

In this instance, absolutely no difference between reference samples and anodes was discernible; consequently all further elucidations apply to both. The observed interactions between slag and refractory material were rather similar for all samples, with one
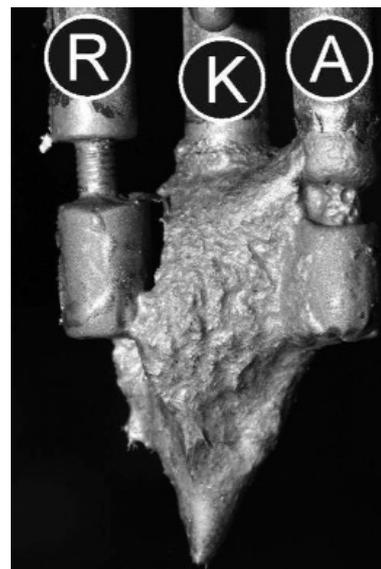

Fig. 4 Cooled electrodes with adhering fayalitic slag after polarization with 5 A for 3 h, 1250 °C (R = reference sample, K = cathode, A = anode)

noticeable exception in the cathodic boundary layer (Fig. 5).

Some reactions between slag and periclase were to be expected, e.g. the formation of olivines or magnesiowustite. Olivines were predominantly identified as interstitial phase, whereas magnesiowustite was the primary phase present at the electrode boundaries. Additionally, unreacted fayalite was found alongside pure wustite. The important difference between reference sample and cathode was the full reduction of the oxidic slag component wustite to metallic iron (Tab. 2). It was thus a reasonable assumption that this reaction played a crucial role in the observed minimization of corrosion at the cathodes.

4 Discussion
4.1 CAS slag

The formation of silicon metal at the cathode was presumably formed through the reduction of silicate complex anions (see ionic theory below) as eq. 1 exemplarily shows.

$$SiO_4^{4-} + 4\,e^- \leftrightharpoons Si_{met} + 4\,O^{2-} \quad (1)$$
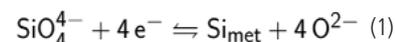
Additionally, oxygen ions stemming from the dissociation of the abundant basic oxide CaO [29] were also present, so the predominant anodic reaction supposedly was the oxidation of oxygen ions according to eq. 2.
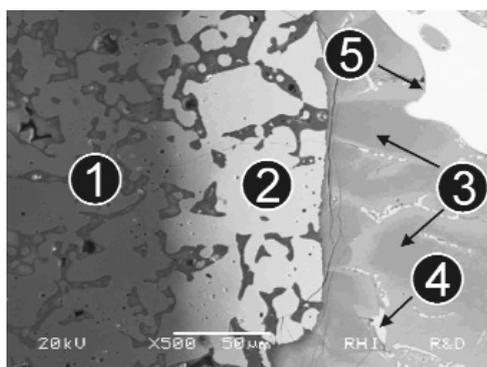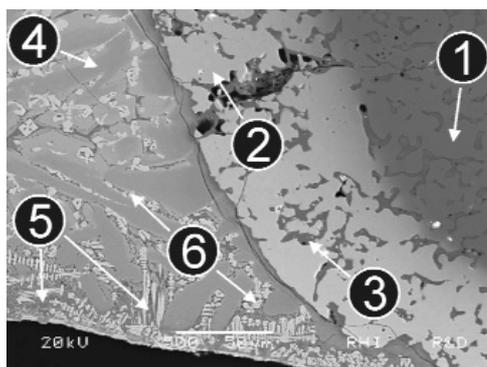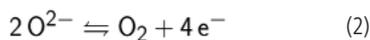
Fig. 5 BSE-SEM-micrographs of the slag-MgO interfacial regions after a 3 h polarization in fayalite slag at 1250 °C with 5 A (~1 V) with a) reference sample, b) cathode; numbers refer to Table 2

$$2\,O^{2-} \leftrightharpoons O_2 + 4\,e^- \qquad (2)$$

The partial reduction of silicate anions to silicon partly deprived the surrounding melt of the oxidic compound, which caused a shift of the local slag composition towards the C_2S primary phase field and thus increased the melt's basicity due to CaO enrichment. However, the electrochemical silicate reduction made only a minor contribution to the overall corrosion protection.

According to the ionic theory of melts slags primarily consist of ions [27]. Therefore, two additional effects were to be expected from the application of electric voltages, the first being the enrichment of Ca^{2+} ions at the cathode boundary. Their considerable mobility surpassed those of complex anions by far and thus resulted in a locally increased CaO content. An analogue conclusion was that the directly opposed diffusion of Mg^{2+} ions into the bulk of the slag due to electrode dissolution should be prevented. The immobilization of Mg^{2+} ions should thus quickly result in a local MgO saturation of the melt at the cathode's edges. At voltages < 8 V neither effect was discernible, which was sup-
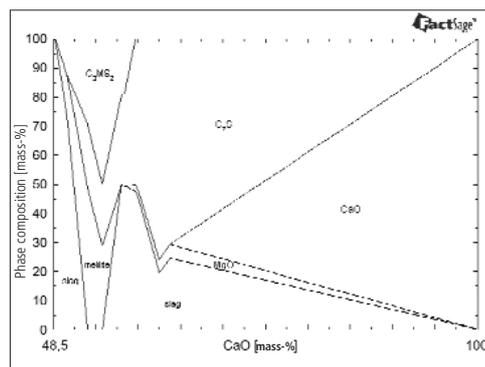

Fig. 6 FactSage calculations for accumulation of Ca^{2+} ions in MgO-saturated cathodic boundary layer in CAS slag at 1400 °C

posedly caused by the superposition of ion-migration by convection.

FactSage calculations were carried out for CaO concentrations from 48,5 % to 100 % to substantiate the assumptions concerning Ca^{2+} enrichment in MgO-saturated boundary layers. First precipitates appeared at CaO concentrations of app. 49 %, with a gradual decrease of the amount of liquid phase to nil (Fig. 6).

For a narrow range of approx. 52–55 % CaO the complete melt solidification with coexisting merwinite, melilite and C_2S was calculated, whereas rather high amounts of liquid phase were again present at CaO contents exceeding 55 %. In short, the calculations mirrored the experiments conducted with 8 and 10 V both.

4.2 Fayalite slag

A pure fayalite slag as used here, allows for straightforward interpretations due to the well documented reactions [32, 33]. The most obvious effect was the formation of metallic iron caused by electrochemical reduction of FeO according to eq. 3.

$$Fe^{2+} + 2\,e^- \leftrightharpoons Fe_{met} \qquad (3)$$
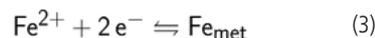
Again, complete dissociation of oxidic compounds into ions was assumed. Pertaining to the anodic reactions there were several possible reactions, none of which could safely be determined.

An obvious reaction again was the already mentioned oxidation of oxygen ions to molecular oxygen according to eq. 1. Due to the high silicate content of the fayalitic-slag system another reaction was likely. Eq. 4 describes the polymerization of single silica

Tab. 2 Phase compositions at the reference sample and the cathode after a 3 h polarization in fayalite slag with a current of 5 A, correspnding to a voltage of 1 V

	MgO	SiO₂	FeO*	Calc. phase composition
	[mass-%]	[mass-%]	[mass-%]	[mass-%]
Reference sample				
1	78,9	-	21,1	Mf
2	21,6	-	78,4	Mf
3	39,2	36,6	24,2	95 Ol (75 M₂S, 25 f₂S) + 5 f
4	-	34,4	65,6	70 f₂S + 30 fS
5	13,6	31,2	55,2	95 Ol (75 f₂S, 25 M₂S) + 5 f
6	-	-	100,0	100 f
Cathode				
1	77,2	-	22,8	Mf
2	24,9	-	75,2	Mf
3	11,6	30,8	57,6	95 Ol (80 f₂S, 20 M₂S) + 5 f
4	-	-	100,0	100 f
5	-	-	100,0	100 metallic Fe

*normalized

tetrahedrons leading to the formation of larger anions as well as the evolution of oxygen [32].

$$2\,SiO_4^{4-} \rightleftharpoons Si_2O_7^{6-} + \tfrac{1}{2}\,O_2 + 2\,e^- \quad (4)$$
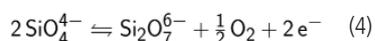
With commonly employed analysis methods like EDS or XRF it was not possible to detect this polymerization process, so above reaction remains a possibility. A more interesting issue was the formation of metallic iron. At 1250 °C all of the formed iron droplets immediately solidified and thereby formed a loose network, which may have well played a role in increasing the slag's viscosity. Appropriate estimations regarding the necessary scope of iron formation are difficult, but *Viswanathan* et al. [42] reported a dramatic viscosity increase in fayalitic slags on reaching a threshold of 7 mass% hematite. Due to the equally high melting point of hematite it is a rather safe assumption to draw parallels to the effect observed in this work.

An additional consideration was the local and permanent removal of the oxidic component FeO from the fayalite slag, resulting in an equally local increase of the silicate content. From the FeO–SiO$_2$ phase diagram [41] it can be easily deduced that the removal of wustite from the slag causes a sharp increase of viscosity owing to the steep slope of the liquidus curve. It also means that the protective effect of applied voltages remains somewhat limited in terms of temperature.

5 Conclusions

In the present work the protection of MgO electrodes in both CAS- and fayalite slags was achieved by cathodic polarization. In both electrolytes a protective slag layer was formed due to different effects. Slag compositions in the CAS system were locally changed at the cathode's edges through rapid migration of small cations such as Ca^{2+}, owing to their high susceptibility to electric fields. The resulting formation of high-melting phases protected the cathode. Conversely the slag basicity at the anode was lowered, which proved detrimental. Accordingly, anodic polarization would prove beneficial only for non-basic electrode materials. Corrosion was also prevented in the fayalitic slag system, where the electrochemical reduction of wustite to metallic iron caused the formation of a highly viscous slag layer. A detrimental factor in both slags was the occurrence of moderate to high current densities, depending on the electrolyte. Current densities in the CAS system increased from approximately 25 mA/cm^2 at 4 V to 175 mA/cm^2 at 8 V. In fayalite slag a further increase of current densities to approx. 4,5 A/cm^2 occurred. Accordingly, economic considerations will ultimately decide on the feasibility of electrochemical corrosion protection measures.

References

[1] Chen, Z.-Y.: Electrochemical corrosion of carbon-containing refractories. China's Refract. 3 (1994) 3–9

[2] Marchant, D.D.; Griffin, C.W; Bates, J.L.: Electrochemical corrosion of iron-magnesium-aluminum spinel in molten potassium salts and coal slag. Am. Ceram. Soc. Bull. 63 (1984) 619–627

[3] Baucke, F.G.K.; Roeth, G.: Electrochemical mechanism of oxygen bubble formation at the interface between oxidic melts and zirconium silicate refractories. Glass Sci. Technol. 61 (1988) 109–118

[4] Iguchi, Y.; Yurek, G.J.; Elliott, J.F.: Electrochemical aspects of refractory attack, in: Proceedings of the 3rd International Iron and Steel Congress, Chicago, ASM, Metals Park, OH, USA, 1979, p. 346–351

[5] Khoroshavin, L.B.; Shcherbatskii, V.B.: An electronic technology for refractories based on the periodic law. Refract. and Ind. Ceram. 46 (2005) 344–351

[6] Videtto, R.B.: Electrochemical approach to refractory-slag corrosion, PhD thesis, Ohio State Univ., Columbus, OH, USA, 1970. p. 169–171

[7] Yoldas, B.E.: Electrochemistry of glass-refractory interfaces and refractory corrosion. PhD thesis, Ohio State Univ., Columbus, OH, USA, 1967, p. 131–133

[8] de Jong, J.: Wetting, electric potential, and corrosion in systems formed by molten glass and refractories. Chem. Weekblad 53 (1957) 517–524

[9] Riaz, S.; Mills, K.C.: Can the application of electric potential increase refractory life?, CFI Ceram. Forum Int. 79 (2002) E47–E50

[10] Riaz, S.; Mills, K.C.; Bain, K.: Experimental examination of slag/refractory interface. Ironmaking Steelmaking 29 (2002) 107–113

[11] Monaghan, B.J.; Nightingale, S.A.; Dong, Q.: The effect of an applied electrical potential on refractory corrosion by slag, in: Proceedings of the 4th International Symposium on Advances in Refractories for the Metallurgical Industries, Hamilton, ON, Canada, 2004, p. 677–686

[12] Hiragushi, K.; Furusato, I.; Shikano H.; Yoshitomi, J.; Kaneko, T.; Mukai, K.: Local corrosion of graphite containing nozzles at powder-metal interface, Taikabutsu Overseas 7 (1987) 4–13

[13] Yoshitomi, J.; Kiwaki, S.; Yagi, T.; Mukai, K.: Local corrosion of blast furnace trough material at the slag-metal interface, Taikabutsu Overseas 7 (1987) 20–23

[14] Mukai, K.; Toguri, J. M.; Stubina, N.M.; Yoshitomi, J.: A mechanism for the local corrosion of immersion nozzles, ISIJ Int. 29 (1989) 469–476

[15] Pilipchatin, L.D.: Dissolution of alumina-silicate refractories in slag melts. Refract. Ind. Ceram. 44 (2003) 219–222

[16] Mukai, K.: Marangoni flows and corrosion of refractory walls. Philos. Trans. Royal Soc. Lond., Ser. A 356 (1998) 1015–1026

[17] Chen, Y.; Brooks, G.A.; Nightingale, S.A.: Slag line dissolution of MgO refractory. Can. Metall. Q. 44 (2005) 323–330

[18] Naruse, Y.; Fujimoto, S.; Harada, T.; Yoshitomi, J.; Hori, M.; Kamiide, M.: Carbon-containing bricks for ladle slag line. Taikabutsu Overseas 4 (1984) 49–57

[19] Pierard, J.; Sichen, D.; Jonsson, P.; Seetharaman, S.; Landin, T.: Effect of slag on carbon bearing MgO refractories. Ironmaking Steelmaking 25 (1998) 374–381

[20] Kim, S.M.; Lu, W.K.: Kinetics and mechanism of the formation of dense magnesium oxide layer in pitch-bearing magnesite brick during service. Metall. Trans. B, 9B (1978) 353–364

[21] Zhao, L.; Sahajwalla, V.: Interfacial phenomena during wetting of graphite/alumina mixtures by liquid iron. ISIJ Int. 43 (2003) 1–6

[22] Aneziris, C.G.; Homola, F.: Electrically assisted high-temperature wettability in oxide and carbon based refractories. Int. Ceram. Rev. 53 (2004) 52–56

[23] Aneziris, C.G.; Homola, F.: Material and process development of advanced refractories for innovative metal processing. Adv. Eng. Mater. 6 (2004) 562–568

[24] Kazakov, A.A.; Matveev, Y.V.; Arykova, L.A.; Ryabov, V.V.: Effect of electric potential on slag impregnation of porous refractories. Metally 4 (1993) 94–96

[25] Frohberg, M.G.; Kapoor, M.L.: Anwendung der Ionentheorie auf die Schlacken umhüllter Elektroden unter besonderer Berücksichtigung der Verteilung von Sauerstoff, Phosphor, Schwefel, Silicium und Mangan zwischen Schlacke und Schweißgut. Schweissen Schneiden 24 (1972) 293–295

[26] Maxl, E.; Hiebler, H.; Presslinger, H.; Antlinger, K.: Microanalytical investigations of oxidizing slags with special consideration of phosphorus- and sulphur-containing phases ISIJ Int. 33 (1993) 88–97

[27] Duffy, J.A.: Chemical bonding in the oxides of the elements: A new appraisal. J. Solid State Chem. 62 (1986) 145–157

[28] Mysen, B.O.: Aluminosilicate systems, structure and properties of silicate melt. Elsevier Science Publishers, Amsterdam, 1988, p. 79–146

[29] Schlackenatlas, Verlag Stahleisen, Düsseldorf, 1981, p. 3–6

[30] Choo, R.T.C.; Toguri, J.M.: The electrodynamic behavior of metal and metal sulfide droplets in slags. Can. Metall. Q. 31 (1992) 113–126

[31] Itoh, S.; Choo, R.T.C.; Toguri, J.M.: Electrocapillary motion of copper and nickel matte droplets on fayalite-based slag surfaces. Can. Metall. Q. 34 (1995) 319–330

[32] Warczok, A.; Riveros, G.; Utigard, T.; Artigas, M.: Electrolysis of liquid fayalite slags. Can. Metall. Q. 44 (2005) 563–570

[33] Warczok, A.; Riveros, G.: Slag cleaning in crossed electric and magnetic fields. Miner. Eng. 20 (2007) 34–43

[34] Kriksunov, L.B.; Jewell, J.M.; Griffin, T.P.; Nagel, C.J.: Strong effects of electrochemical polarization on corrosion of ceramics in molten glass, in: Proceedings of the 11th International Symposium on Molten Salts, San Diego, CA, USA, 1998, p. 435–447

[35] Sauerbrey, R.K.; Mori, G.; Majcenovic, Ch.; Harmuth, H.: Corrosion protection of MgO electrodes at 1400 °C. Corros. Sci. 51 (2009) 1–5

[36] Siegl, W.: Electrochemical reaction at magnesia carbon bricks in the conductive bottom of d.c.-arc urnaces. Radex Rundschau (1992) 208–216

[37] Kazakov, A.A.: Influence of the electrical potential on converter smelting. Metally 6 (1997) 25–28

[38] Schlackenatlas, Verlag Stahleisen, Düsseldorf, 1981, p. 267

[39] Schlackenatlas, Verlag Stahleisen, Düsseldorf, 1981, p. 264

[40] Schwiete, H.E.; Krönert, W.; Deckert, K.: Existenzbereiche und Stabilisierung von Hochtemperaturmodifikationen des Dicalciumsilicates. Zement-Kalk-Gips (1968) 359–366.

[41] Routschka, G. [Ed.]: Einführung, in: Taschenbuch Feuerfeste Werkstoffe, 3rd ed., Vulkan-Verlag, Essen, 2001, p. 8–9

[42] Viswanathan, N.N.; Ji, F.-Z.; Sichen, D.; Seetharaman, S.: Viscosity measurements on some fayalitic slags. ISIJ Int. 41 (2001) 722–727